The Journal of Chemical Physics

RESEARCH ARTICLE | SEPTEMBER 26 2017

Translation-rotation decoupling of tracers of locally favorable structures in glass-forming liquids

Yoonjae Park; Jeongmin Kim; Bong June Sung

J. Chem. Phys. 147, 124503 (2017)
https://doi.org/10.1063/1.4994643

Translation-rotation decoupling of tracers of locally favorable structures in glass-forming liquids

Yoonjae Park, Jeongmin Kim, and Bong June Sung[a)]
Department of Chemistry, Sogang University, Seoul 121-742, South Korea

(Received 6 July 2017; accepted 8 September 2017; published online 26 September 2017)

Particles in glass-forming liquids may form domains of locally favorable structures (LFSs) upon supercooling. Whether and how the LFS domains would relate to the slow relaxation of the glass-forming liquids have been issues of interest. In this study, we employ tracers of which structures resemble the LFS domains in Wahnström and Kob-Andersen (KA) glass-forming liquids and investigate the translation-rotation decoupling of the tracers. We find that the tracer structure affects how the translation and the rotation of tracers decouple and that information on the local mobility around the LFS domains may be gleaned from the tracer dynamics. According to the Stokes-Einstein relation and the Debye-Stokes-Einstein relation, the ratio of the translational (D_T) and rotational (D_R) diffusion coefficients is expected to be a constant over a range of T/η, where η and T denote the medium viscosity and temperature, respectively. In supercooled liquids and glasses, however, D_T and D_R decouple due to dynamic heterogeneity, thus D_T/D_R not being constant any more. In Wahnström glass-forming liquids, icosahedron LFS domains are the most long-lived ones and the mobility of neighbor particles around the icosahedron LFS domain is suppressed. We find from our simulations that the icosahedron tracers, similar in size and shape to the icosahedron LFS domains, experience drastic translation-rotation decoupling upon cooling. The local mobility of liquid particles around the icosahedron tracers is also suppressed significantly. On the other hand, tracers of FCC and HCP structures do not show translation-rotation decoupling in the Wahnström liquid. In KA glass-forming liquids, bicapped square antiprism LFS domains are the most long-lived LFS domains but are not correlated significantly with the local mobility. We find from our simulations that D_T and D_R of bicapped square antiprism tracers, also similar in size and shape to the bicapped square antiprism LFS domains, do not decouple significantly similarly to tracers of other structures, thus reflecting that the local mobility would not be associated strongly with LFS domains in the KA liquid. *Published by AIP Publishing.* https://doi.org/10.1063/1.4994643

I. INTRODUCTION

The dynamics of glass-forming liquids slows down dramatically and becomes heterogeneous upon supercooling.[1–17] Supercooled liquids consist of regions of different mobility: molecules in some regions diffuse fast while molecules in other regions hardly diffuse. Such intriguing dynamic behaviors have been also observed in biological systems such as cell cytoplasm[18–24] and cell membranes:[25–28] the protein diffusion was slow, subdiffusive, and spatially heterogeneous. Understanding the mechanism for the slow relaxation and the dynamic heterogeneity should be, therefore, an issue of importance, but still remains a challenge. There has been especially no consensus on whether there exists a structural origin for the slow relaxation of the supercooled liquids.[29–44] It is partly because of the lack of simulation and experimental tools to investigate various kinds of glass-forming liquids. For example, it is formidable in experiments to identify a structural motif in various glass-forming liquids and investigate how the structural motif would relate to the mobility. In this paper, we show that the translation-rotation decoupling of tracer molecules, one of the signatures of supercooled liquids, may be used as a measure to obtain the information on how local structure relates to local mobility.

Several structural motifs are found in supercooled liquids, some of which are relatively stable and form the domains of locally favorable structures (LFSs).[29,45–55] For example, icosahedron and bicapped square antiprism (BSA) are long-lived LFSs observed in Wahnström and Kob-Andersen (KA) glass-forming liquids, respectively. The LFS domains grow significantly upon supercooling such that the long-lived LFS domains even construct a percolating network at a sufficiently low temperature. This indicates that the growth of LFS domains might relate to the slow relaxation of supercooled liquids. But the formation of the percolating network does not necessarily imply structural arrest because the lifetime of LFS domains is finite. Therefore, how LFS domains affect the local mobility is still an open and important question. A recent study showed that icosahedron LFSs in the Wahnström liquid lowered the mobility of neighbor particles around the icosahedron LFSs.[29,32,47] On the other hand, other studies illustrated that LFS domains in the KA liquid were not strongly correlated with the mobility.[56]

[a)]Author to whom correspondence should be addressed: bjsung@sogang.ac.kr

Both the Stokes-Einstein (SE) relation and the Debye-Stokes-Einstein (DSE) relation originate from the fluctuation-dissipation theorem, which relates the translational (D_T) and rotational (D_R) diffusion coefficients of colloids to a balance between thermal fluctuation (k_BT) and friction (η). Here, k_B, η, and T denote the Boltzmann constant, medium viscosity, and temperature, respectively. In homogeneous solutions, $D_T \sim k_BT/\eta$ and $D_R \sim k_BT/\eta$. This implies that D_T and D_R should couple: if the value of η were to be doubled (for example, by introducing viscogens), both D_T and D_R should be halved. Therefore, the ratio of D_T/D_R should remain constant over a range of T/η. In supercooled liquids and glasses, however, the diffusion becomes spatially heterogeneous such that the decoupling of the translation and rotation of colloids occurs. In some cases, the SE relation breaks down[1,57–59] while the DSE relation holds. D_T displays the fractional viscosity dependence of $D_T \sim (\eta/T)^{-\xi}$ with $\xi < 1$ such that D_T/D_R does not remain constant any more. In other cases, the DSE relation breaks[60–67] and D_R displays the fractional viscosity dependence, thus resulting in decoupling. In this study, we investigate the translation-rotation decoupling of tracers of different shapes [icosahedron,[68] bicapped square antiprism (BSA), FCC, and HCP[69]] in glass-forming liquids. We find that whether the decoupling occurs or not depends strongly on the tracer structure.

The long time translational diffusion coefficient (D_T) of a colloid (or a tracer) may be obtained only after the tracer diffuses through several domains of different mobility in supercooled liquids. In such a case, the translational relaxation does not occur in one domain but the tracer diffusion enters a Fickian regime[70–76] after several domains emerge and disappear. D_T should be, therefore, a measure of the overall mobility of the supercooled liquids. On the other hand, the rotational relaxation (and D_R) of a tracer is sensitive to the local mobility around the tracer in supercooled liquids. If the local mobility around tracers were to be different significantly from the overall mobility of supercooled liquids, the DSE relation would break down and the translation-rotation decoupling would occur. Then, the trend of the translation-rotation decoupling may be employed to investigate the local mobility around the tracer in supercooled liquids.

We take an advantage of tracers that resemble LFSs and investigate their trend of translation-rotation decoupling. In case the translation-rotation decoupling is sensitive to the local mobility around the tracer, the decoupling trend would reveal how LFSs would affect the local mobility. We find that D_T and D_R of icosahedron tracers decouple significantly in Wahnström liquids because D_R shows fractional viscosity dependence. On the other hand, the bicapped square antiprism tracers do not display decoupling in KA liquids, which is consistent with previous observations that the bicapped square antiprism LFS was not correlated strongly with the mobility.[56] Our simulation results suggest that investigating the translation-rotation decoupling of tracers of LFSs would be an indirect but feasible route to studying the relation between LFSs and local mobility. It is usually formidable in experiments to identify LFS domains, measure, and investigate the local mobility around LFSs. Because the translation-rotation decoupling is associated with the correlation between LFS domains and local mobility, one may obtain information on the local mobility from the studies on the translation-rotation decoupling.

The rest of this paper is organized as follows. Our model and simulation details are described in Sec. II. Simulation results are discussed in Sec. III and Sec. IV contains the summary and conclusions.

II. MODELS AND METHODS

A. Models for glass-forming liquids

We consider two different glass-forming liquids: Wahnström[77] and Kob-Andersen (KA)[78–80] glass-forming liquids. The Wahnström liquid is an equimolar binary mixture of A and B particles. Our simulation systems for the Wahnström liquid are composed of 12000 particles. A and B particles interact via a truncated and shifted Lennard-Jones (LJ) potential as follows:

$$U_{\alpha\beta}(r) = 4\epsilon_{\alpha\beta}\left[\left(\frac{\sigma_{\alpha\beta}}{r}\right)^{12} - \left(\frac{\sigma_{\alpha\beta}}{r}\right)^{6}\right] - U_c, r < r_c$$
$$= 0, r > r_c. \quad (1)$$

Here, r is the distance between two particles, and $(\alpha, \beta) \in \{A, B\}$. $\epsilon_{\alpha\beta} = \epsilon$ for all pairs of particles, i.e., $\epsilon_{AA} = \epsilon_{AB} = \epsilon_{BB} = \epsilon$. ϵ is taken as an energy unit. In this study, the diameter and the mass of A particles are used as the units of length and mass, respectively, i.e., $\sigma_{AA} = \sigma$ and $m_A = m$. $\sigma_{AB} = 1.1\sigma$ and $\sigma_{BB} = 1.2\sigma$ are used for simulations. The mass of a B particle is $2m$. The time unit is, then, $\tau = \sqrt{m\sigma^2/\epsilon}$.

The KA liquid is an 80:20 binary mixture of A and B particles. The masses of A and B particles for the KA liquid are identical ($m_A = m_B = m$). Particles in KA liquids also interact via the identical form of the truncated and shifted LJ potential but with different interaction parameters: $\sigma_{AA} = \sigma$, $\sigma_{AB} = 0.8\sigma$, $\sigma_{BB} = 0.88\sigma$, $\epsilon_{AA} = \epsilon$, $\epsilon_{AB} = 1.5\epsilon$, and $\epsilon_{BB} = 0.5\epsilon$. We construct simulation systems for the KA liquid by using 12000 particles.

We employ four different types of tracers [icosahedron, bicapped square antiprism (BSA), HCP, and FCC]. Three types of tracers except bicapped square antiprism tracers are composed of 12 spherical particles of diameter σ and mass m. Bicapped square antiprism tracers are composed of 11 spherical particles. The intramolecular interaction between particles within a single tracer is described by using both a harmonic bond potential ($U_b(r) \equiv 100\epsilon(r - r_0)^2$) and a harmonic angle ($U_a(\theta) \equiv 100\epsilon(\theta - \theta_0)^2$) potential. Here, θ denotes an angle between two bonding vectors of three neighbor particles. θ_0 is the value of θ at a potential energy minimum. For icosahedron and bicapped square antiprism tracers, θ_0 is 60° and 90°, respectively. For HCP and FCC tracers, on the other hand, θ_0 is either 60° or 90° (Fig. 1). There are 60 angles in a single tracer for icosahedron, 8 angles in bicapped square antiprism tracers, and 48 angles for HCP and FCC tracers. r_0 used in this study corresponds to the position of the first peak of the radial distribution function of liquids. The force constants of 100ϵ for U_b and U_a are large enough to maintain the structures of tracers during our simulations. The particles of a tracer interact with other particles (that do not belong to the tracer) via $U_{\alpha\beta}(r)$.

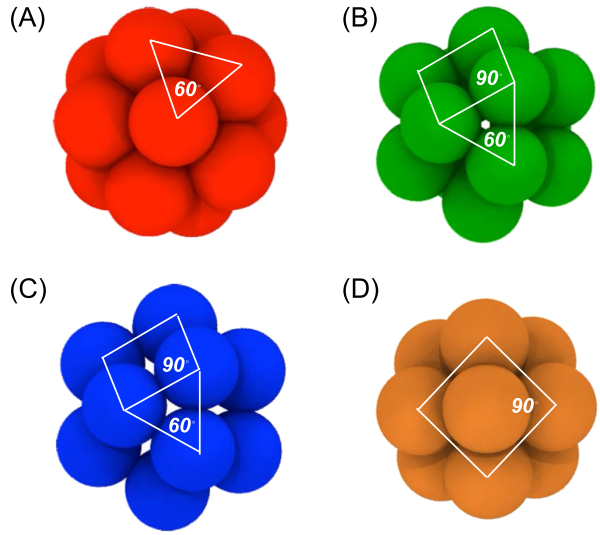

FIG. 1. Four different types of tracers used in this study: (a) icosahedron (red), (b) FCC (green), (c) HCP (blue), and (d) bicapped square antiprism (BSA) (orange) tracers. Angles in figures indicate the values of θ_0 used in simulations.

The radii of the tracers in this study are almost 1.5σ except BSA. In the case of BSA, the distance between its center of mass and its constituent particle ranges from 1.36 to 1.68σ. We estimate the asphericity (δ^*) defined as follows:[81]

$$\delta^* = 1 - 3\frac{\lambda_1^2\lambda_2^2 + \lambda_2^2\lambda_3^2 + \lambda_1^2\lambda_3^2}{(\lambda_1^2 + \lambda_2^2 + \lambda_3^2)^2}, \tag{2}$$

where λ_1, λ_2, and λ_3 are the eigenvalues of gyration tensors of tracers. δ^* ranges from 0 to 1 and $\delta^* \approx 0$ for spherical tracers. In this study, the values of δ^* are all close to zero ($\delta^* \approx 0.002$ for icosahedron, FCC, and HCP tracers and $\delta^* = 0.069$ for BSA), indicating that our tracers are of spherical shape.

B. Molecular dynamics simulations

Initial configurations for simulations are generated by inserting 2 tracers and 12000 particles at random positions in a primary simulation cell. If any overlap between particles occurs, we discard the configuration and try new random positions for the particles. The dimension ($L \equiv (N/\rho)^{1/3}$) of the cubic simulation cell is about 25.1σ in Wahnström liquids and 21.6σ in KA liquids. N is the total number of particles including tracer particles. ρ is the number density, which is 0.75 in Wahnström liquids and 1.2 in KA liquids. Initial velocities for particles are sampled randomly from the Maxwell-Boltzmann velocity distribution with zero total momentum.

We perform canonical molecular dynamics (MD) simulations by employing the LAMMPS simulator with a velocity-Verlet integrator and Nosé-Hoover thermostat.[82] The time step for MD simulations is 0.001τ, and periodic boundary conditions are applied in all directions. We equilibrate systems by performing MD simulations at least 1000 times longer than the translational relaxation time (τ_T) of tracers. We change T from 2 to 0.6 for the Wahnström liquid and from 2 to 0.485 for the KA liquid. Because the onset temperature T_0 and the critical temperature T_c is $(T_0, T_c) = (0.8, 0.55)$ for the Wahnström liquid and $(T_0, T_c) = (1, 0.435)$ for the KA liquid, $T = 0.6$ for the Wahnström liquid and $T = 0.485$ for the KA liquid are sufficiently low temperatures at which dynamic heterogeneity is significant.

We estimate the mean-square displacement ($\langle(\Delta\vec{r}(t))^2\rangle$) and the non-Gaussian parameter ($\alpha_2(t)$) of Wahnström and Kob-Andersen (KA) liquids as follows:

$$\langle(\Delta\vec{r}(t))^2\rangle = \langle|\vec{r}(t) - \vec{r}(0)|^2\rangle, \tag{3}$$

$$\alpha_2(t) = \frac{3\langle(\Delta\vec{r}(t))^4\rangle}{5\langle(\Delta\vec{r}(t))^2\rangle^2} - 1, \tag{4}$$

where $\vec{r}(t)$ is the position vector of the particles of Wahnström and Kob-Andersen (KA) liquids at time t. $\langle\cdots\rangle$ denotes an ensemble average over all particles in the system.

The mean-square displacement ($\langle(\Delta\vec{r}(t))^2\rangle_t$) and the translational diffusion coefficient (D_T) of tracers are also estimated, i.e.,

$$\langle(\Delta\vec{r}(t))^2\rangle_t = \langle|\vec{r}_{com}(t) - \vec{r}_{com}(0)|^2\rangle, \tag{5}$$

$$D_T = \lim_{t\to\infty}\frac{\langle(\Delta\vec{r}(t))^2\rangle_t}{6t}, \tag{6}$$

where $\vec{r}_{com}(t)$ is the position vector of the center of mass of a tracer at time t. We also estimate the mean-square angular displacement ($\langle(\Delta\vec{\varphi}(t))^2\rangle$)[57] and the rotational time correlation function ($U(t)$) of tracers as follows:

$$\langle(\Delta\vec{\varphi}(t))^2\rangle = \langle|\vec{\varphi}(t) - \vec{\varphi}(0)|^2\rangle, \tag{7}$$

$$U(t) = \frac{\langle\vec{u}(t)\cdot\vec{u}(0)\rangle}{|\vec{u}(0)\cdot\vec{u}(0)|}, \tag{8}$$

where $\vec{u}(t)$ is a normalized vector that points one particle of a tracer at its perimeter from the center of mass of the tracer. We investigate the rotation of the tracer by tracking the vector $\vec{u}(t)$. $\vec{\varphi}(t)$ is the unbounded angle vector of $\vec{u}(t)$ given by $\vec{\varphi}(t) = \vec{u}(0)\times\vec{u}(t)$. The rotational diffusion coefficient (D_R) of tracers can be obtained by using either $\langle(\Delta\vec{\varphi}(t))^2\rangle$ (Einstein formalism) or $U(t)$ (Debye formalism). In the Einstein formalism, $D_R = \lim_{t\to\infty}\langle(\Delta\vec{\varphi}(t))^2\rangle/(4t)$ is used. In the Debye formalism, on the other hand, we calculate the rotational relaxation time (τ_R) of $U(t)$ by using the relation $U(t = \tau_R) = 1/e$ and estimate $D_R = 1/(2\tau_R)$.

C. Topological cluster classification

We employ the topological cluster classification (TCC)[83] analysis to investigate the local structure of Wahnstöm and Kob-Andersen (KA) liquids. TCC analysis detects the minimum energy clusters made of 5 to 13 particles and allows us to investigate high-order local structures in supercooled liquids. The first step of the TCC analysis is to estimate bonds between pairs of neighbor particles. The bonds are identified using a modified Voronoi construction with a four-membered parameter (f_c) and a maximum bond length cutoff (r_c), which were used in previous studies to detect long-lived clusters in Lennard-Jones fluids.[47,48,83] In this study, we use (f_c, r_c) = (0.82, 1.62σ) for Wahnstöm liquids and (f_c, r_c) = (1, 2σ) for KA liquids. The shortest-path rings composed of 3 to 5 particles are, then, searched within the bond network. These shortest-path rings define the basic clusters. By either combining basic clusters or adding a few bonded particles to these

clusters, larger clusters are determined. We compare the bond network of each cluster with those of the minimum energy clusters and assign the topology to the cluster.

According to a recent study,[47] the fraction of liquid particles that belong to each local structure, in general, increased with a decrease in the temperature T. Some clusters maintained their structure for sufficiently long times, while other clusters were broken due to thermal fluctuation before the translational relaxation time. In the Wahnstöm liquid, 13-membered icosahedron was a long-lived locally favorable structure and crystalline structures (FCC and HCP) were short lived structures. In the case of the KA liquid, 11-membered bicapped square antiprism was a long-lived locally favorable structure, while icosahedron and FCC structures were relatively short lived structures.

III. RESULTS AND DISCUSSIONS

A. The diffusion and dynamic domains of glass-forming liquids

Wahnström and KA glass-forming liquids have been investigated extensively in previous studies.[37,39,45–48,56,77,78] In this subsection, we investigate whether the presence of tracers would influence the structure and dynamics of the glass-forming liquids. We find that $g(r)$, $\langle(\Delta\vec{r}(t))^2\rangle$, and $\alpha_2(t)$ of glass-forming liquids are hardly sensitive to the presence of tracers of any kind. This indicates that the tracers employed in this study would be proper stand-ins to examine the glass-forming liquids.

Figure 2 depicts $\langle(\Delta\vec{r}(t))^2\rangle$ of Wahnström and KA liquids with and without tracers. For a given temperature T, the presence of tracers does not affect $\langle(\Delta\vec{r}(t))^2\rangle$. $\langle(\Delta\vec{r}(t))^2\rangle$ at a high temperature of $T = 2$ enters a Fickian regime ($\langle(\Delta\vec{r}(t))^2\rangle \sim t^1$) quickly after a short ballistic regime ($\langle(\Delta\vec{r}(t))^2\rangle \sim t^2$). As T is decreased, a subdiffusive regime develops with $\langle(\Delta\vec{r}(t))^2\rangle \sim t^\alpha$ and $\alpha < 1$. The subdiffusive regime becomes longer at a lower temperature. In the case of Wahnström liquids at $T = 0.65$, the subdiffusive regime lasts for about two orders of magnitude of times before a Fickian regime appears. Such a subdiffusive behavior of $\langle(\Delta\vec{r}(t))^2\rangle$ has been observed in various glass-forming liquids.

The glass-forming liquids often display non-Gaussian dynamics at low temperatures, which is characterized by the non-Gaussian parameter $\alpha_2(t)$. $\alpha_2(t)$ for glass-forming liquids is usually very negligible at short times but increases sharply when the dynamic heterogeneity begins to appear at intermediate time scales. Once $\alpha_2(t)$ reaches its maximum value, $\alpha_2(t)$ decays back to zero. $\alpha_2(t)$ usually reaches its maximum right before $\langle(\Delta\vec{r}(t))^2\rangle$ enters the Fickian regime, which corresponds to the time when the dynamic heterogeneity is the most significant.

Figure 3 depicts $\alpha_2(t)$ of Wahnström and KA liquids with and without tracers. $\alpha_2(t)$ at $T = 2$ is quite small compared to those at low temperatures, thus implying that the liquid diffusion should be Gaussian at $T = 2$. As T is decreased, $\alpha_2(t)$ is increased significantly. For example, $\alpha_2(t)$ reaches about 1 at $t \approx 100$ for the Wahnström liquid without tracers at $T = 0.65$, thus indicating that the Wahnström liquid diffusion becomes

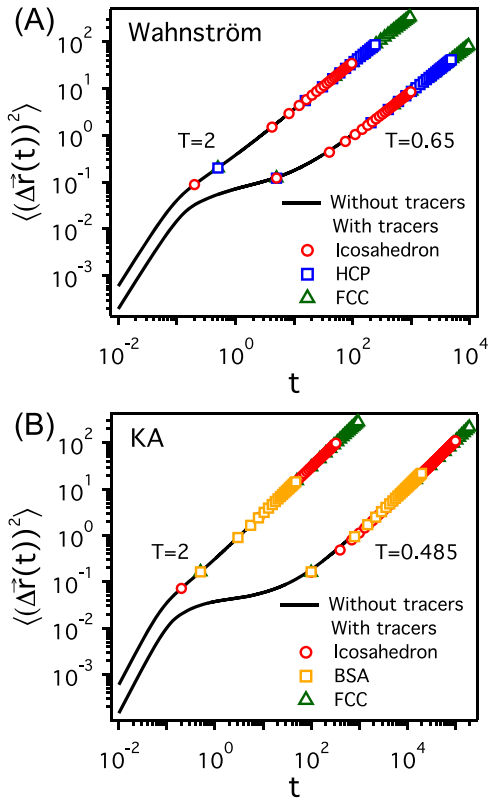

FIG. 2. Mean-square displacements $\langle(\Delta\vec{r}(t))^2\rangle$ of (a) Wahnström particles (A particles) and (b) KA particles (A particles) at various temperatures with and without tracers. BSA indicates bicapped square antiprism tracers.

quite non-Gaussian at $t = 100$. When tracers are inserted into the liquids, $\alpha_2(t)$ is increased slightly: $\alpha_2(t)$ is increased by about 10% at the peak position of $\alpha_2(t)$. This may be attributed to our observation that the local mobility around the tracer is decreased (Fig. 11). The peak position of $\alpha_2(t)$ (the time when the dynamic heterogeneity is significant), however, does not change with the presence of tracers.

Figure 4 depicts the radial distribution functions ($g(r)$) of particles of both Wahnström and KA glass-forming liquids with and without tracers at $T = 2$. $g(r)$ is not affected by the presence of tracers at all temperatures in this study. Because the tracer concentration is quite small in this study, the presence of tracers does not interrupt the overall structure (at least the second order correlation) of particles of glass-forming liquids.

B. Structure of glass-forming liquids around tracers

Icosahedron and bicapped square antiprism are long-lived locally favorable structures (LFSs) in Wahnström and KA liquids, respectively. Previous studies showed that the clusters of LFSs grew upon supercooling and formed percolating networks.[35,45–48] The percolating networks were, however, transient. It remains unanswered whether and how the percolating networks would lead to the slow-down of the relaxation of glass-forming liquids.

We perform topological cluster classification (TCC) analysis for configurations obtained from MD simulations. We also find that icosahedron and bicapped square antiprism clusters grow in Wahnström and KA liquids, respectively, as T is

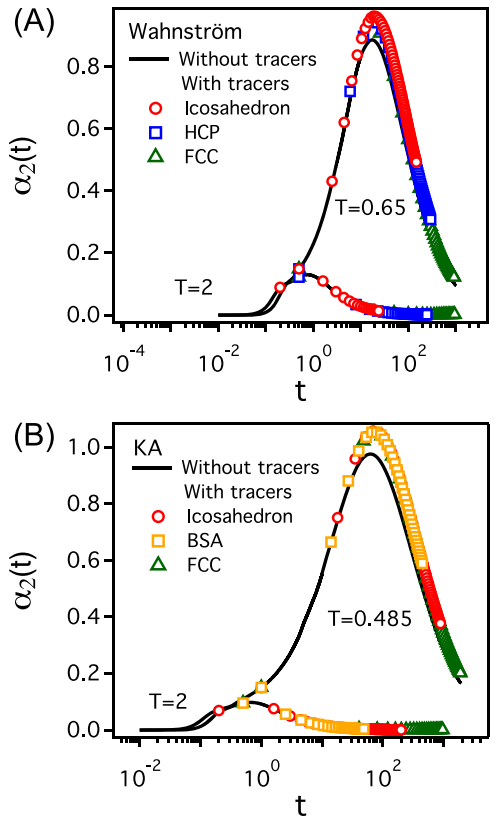

FIG. 3. Non-Gaussian parameter $\alpha_2(t)$ of (a) Wahnström particles (A particles) and (b) KA particles (A particles) at various temperatures with and without tracers.

decreased. Figures 5(a) and 5(c) depict the fractions ($f_{overall}$) of all liquid particles that participate in icosahedron, bicapped square antiprism, HCP, and FCC clusters with and without tracers of different shapes. Figures 5(b) and 5(d) depict the fractions (f_{local}) of local neighbor particles around tracers (of various kinds) that participate in icosahedron, bicapped square antiprism, HCP, and FCC clusters.

In the Wahnström liquid, HCP and FCC clusters hardly grow with a decrease in T. On the other hand, the overall fraction ($f_{overall}$) of particles that belong to icosahedron clusters increases sharply upon cooling [Fig. 5(a)]. Interesting is that

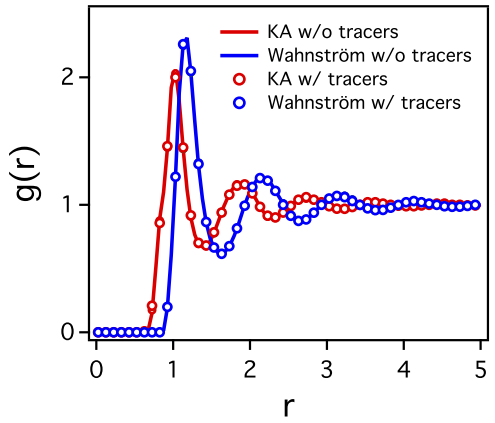

FIG. 4. Radial distribution function $g(r)$ of Wahnström particles (blue) and KA particles (red) at $T = 2$ with (symbols) and without (lines) tracers.

the presence of tracers hardly changes $f_{overall}$. In Fig. 5(a), different symbols represent different types of tracers in the liquid and different colors represent LFSs of different structures: red, blue, orange, and green lines for icosahedron, HCP, bicapped square antiprism (BSA), and FCC LFSs, respectively. $f_{overall}$'s of each LFS without tracers are depicted with filled diamond symbols. For example, $f_{overall}$'s of icosahedron clusters (red lines) in the Wahnström liquid with (open symbols) and without (filled symbols) tracers overlap well with one another.

A similar trend is observed in KA liquids [Fig. 5(c)]. As T is decreased, bicapped square antiprism (BSA) clusters, which are long-lived LFSs in the KA liquid, grow more significantly than FCC and icosahedron clusters. FCC clusters hardly grow. Even in the KA liquid, the presence of tracers does not change $f_{overall}$ for clusters significantly. Note that $f_{overall}$ of the long-lived LFSs (icosahedron clusters) in the Wahnström liquid increases up to 20%, whereas $f_{overall}$ of the long-lived LFSs (bicapped square antiprism clusters) in the KA liquid increases only by about 12%.

Icosahedron tracers induce the formation of icosahedron clusters in the Wahnström liquid, whereas bicapped square antiprism tracers do not in the KA liquid. We estimate the local fraction (f_{local}) of liquid particles around tracers that participate in the clusters of different structures. We consider liquid particles that are located within the distance of 3σ from the center of mass of tracers. The distance of 3σ corresponds to the 2nd peak position of the pair correlation function of liquid particles and tracers. Figures 5(b) and 5(d) depict the fraction (f_{local}) of local liquid particles around tracers that participate in icosahedron, bicapped square antiprism (BSA), FCC, and HCP LFSs. In Figs. 5(b) and 5(d), different symbols represent different types of tracers present in the liquid, whereas different colors represent LFS clusters of different structures: red, blue, orange, and green lines for icosahedron, HCP, bicapped square antiprism (BSA), and FCC liquid clusters just like in Figs. 5(a) and 5(c).

It is interesting that about 40% of local Wahnström particles around icosahedron tracers become the parts of icosahedron clusters, i.e., $f_{local} \approx 0.4$ [Fig. 5(b)] at $T = 0.6$. Considering that the overall fraction ($f_{overall}$) of Wahnström particles in icosahedron LFSs is about 20% at $T = 0.6$ [Fig. 5(a)], this indicates that icosahedron tracers induce the formation of icosahedron LFSs around themselves significantly. Around HCP and FCC tracers in the Wahnström liquid, about 20% of Wahnström particles participate in icosahedron clusters ($f_{local} \approx 0.2$), which is close to $f_{overall}$ of Wahnström particles in icosahedron structures. Tracers in the Wahnström liquid do not facilitate the formation of HCP and FCC clusters.

In the KA liquid, even the bicapped square antiprism tracers, which resemble a long-lived LFS domain, does not promote the formation of any kind of clusters. The fraction of KA particles around tracers (of any kind) that participate in a particular structure is almost identical to the overall fraction of KA particles in the structure, i.e., $f_{local} \approx f_{overall}$ [Fig. 5(d)]. This indicates that even though the bicapped square antiprism structure is a long-lived LFS in the KA liquid, it might not induce any structural change locally.

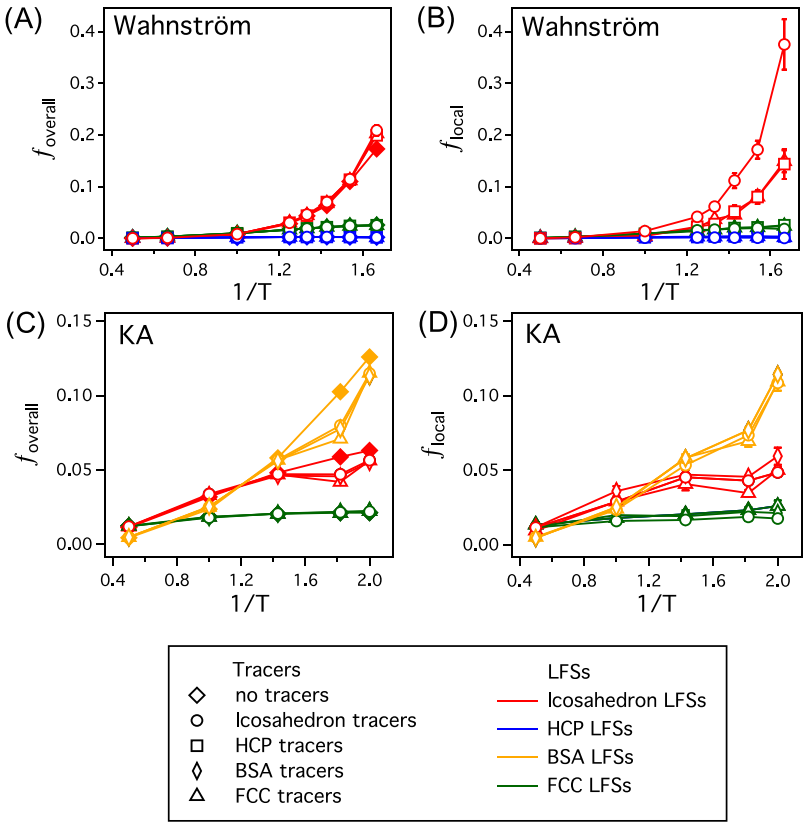

FIG. 5. Topological cluster classification analysis: the fraction of [(a) and (b)] Wahnström and [(c) and (d)] KA particles that belong to each LFS. (a) and (c) represent the fraction of all liquid particles, and (b) and (d) represent the fraction of local particles around tracers. The different symbols represent tracers of different shapes present in the liquid while different colors represent different local structures that liquid particles belong to. Filled symbols represent the fraction of all liquid particles when tracers are not inserted. For example, red circles in (b) represent the fraction of local liquid particles around icosahedron tracers that belong to icosahedron LFS domains. Orange triangles in (c) represent the fraction of liquid particles that belong to bicapped square antiprism (BSA) LFS domains in the KA liquid with FCC tracers.

C. The translation and rotation of tracers

Tracers enter the Fickian regime ($\langle(\Delta\vec{r}(t))^2\rangle_t \sim t^1$) quickly at high temperatures but display a subdiffusive regime at low temperatures. Tracers enter the Fickian regime much later than liquid particles due to the large tracer size. For example, when $T = 0.65$, icosahedron tracers in the Wahnström liquid enter the Fickian regime at $t \approx 600$, while Wahnström particles enter the Fickian regime at $t \approx 50$.

Interesting is that the tracer diffusion depends on the structure of tracers even though the tracer sizes are similar. In the case of the Wahnström liquid, as T is decreased, the diffusion of icosahedron tracers is suppressed more than HCP and FCC tracers [Fig. 6(a)]. For a given T, $\langle(\Delta\vec{r}(t))^2\rangle_t$ of HCP and FCC tracers are almost identical to each other. The dependence of $\langle(\Delta\vec{r}(t))^2\rangle_t$ on the tracer shape in the KA liquid is not as significant as in the Wahnström liquid. However, the translational diffusion of FCC tracers in the KA liquid is slightly slower than those of icosahedron and bicapped square antiprism tracers [Fig. 6(b)].

At sufficiently low temperatures, the rotational diffusion of tracers is more sensitive to the tracer shape than the translational diffusion. Our simulation results show that at a high temperature of $T = 2$, $\langle(\Delta\vec{\varphi}(t))^2\rangle$'s of different types of tracers are almost identical to one another (Fig. 7). Because tracers in this study are almost spherical with $\delta^* \approx 0$, the DSE relation should hold at $T = 2$. At low temperatures, on the other hand, the DSE relation breaks down and $\langle(\Delta\vec{\varphi}(t))^2\rangle$ is sensitive to the tracer shape. In the case of the Wahnström liquid [Fig. 7(a)] at $T = 0.65$, $\langle(\Delta\vec{\varphi}(t))^2\rangle$ of icosahedron tracers is smaller by about an order of magnitude than those of HCP and FCC tracers. Similarly in the KA liquid at $T = 0.485$, $\langle(\Delta\vec{\varphi}(t))^2\rangle$ of FCC tracers is smaller than those of icosahedron and bicapped square antiprism (BSA) tracers. A recent simulation study by Taamalli *et al.*[84] showed that not only the

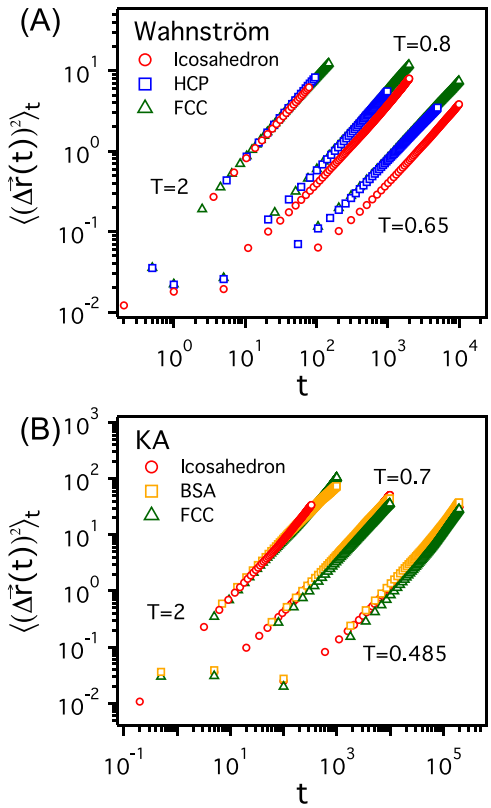

FIG. 6. Mean-square displacements $\langle(\Delta\vec{r}(t))^2\rangle_t$ of tracers in (a) the Wahnström liquid and (b) the KA liquid at various temperatures.

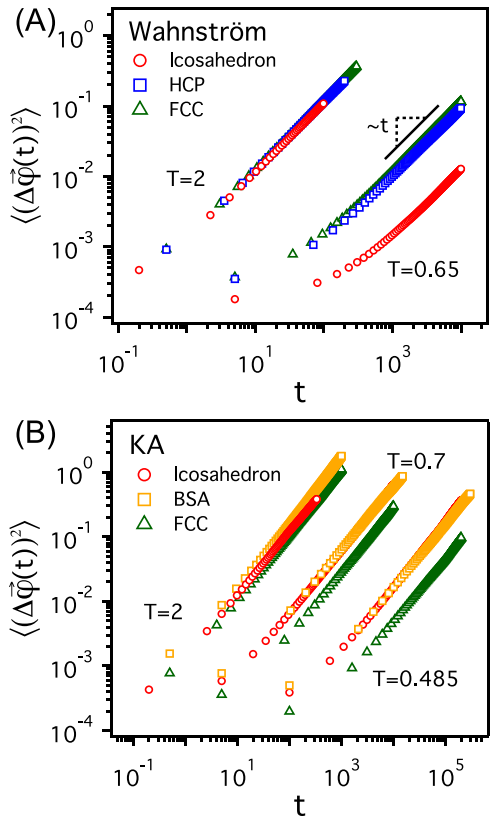

FIG. 7. Mean-square angular displacements $\langle(\Delta\vec{\varphi}(t))^2\rangle$ of tracers in (a) the Wahnström liquid and (b) the KA liquid at various temperatures.

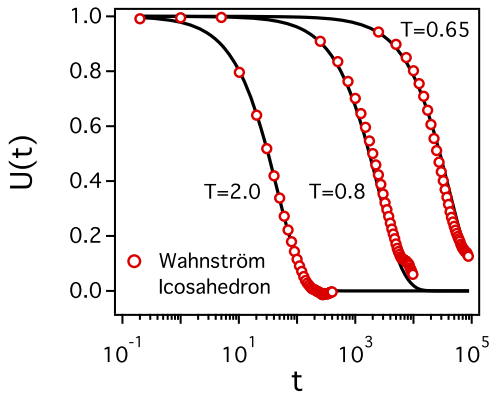

FIG. 8. Rotational time correlation functions $U(t)$ of icosahedron tracers in the Wahnström liquid (red symbols) at various temperatures. Lines are drawn with the equation $U(t) = \exp(-2D_R t)$ with D_R obtained from $\langle(\Delta\vec{\varphi}(t))^2\rangle$ and the Einstein formalism.

shape but also the size of tracers would make a qualitative difference in the dynamic heterogeneity of liquid particles. Since all types of tracers in this study are similar in size, the differences in translational diffusion and rotational diffusion among tracers may not be attributed to the size of tracers in our simulations.

Because the rotational diffusion of all tracers in this study enters the Fickian regime ($\langle(\Delta\vec{\varphi}(t))^2\rangle \sim t^1$) even at low temperatures, D_R of tracers can be estimated readily by employing the Einstein relation, i.e., $D_R \equiv \lim_{t\to\infty}\langle(\Delta\vec{\varphi}(t))^2\rangle/(4t)$. However, previous simulation studies reported several cases where D_R of the Einstein formalism differed significantly from D_R of the Debye formalism, which made the study on the translation-rotation decoupling complicated.[60,62] In the case of the Debye formalism, the rotational correlation function $U(t)$ is obtained from simulations and is fitted to the exponential function, $\exp(-2D_R t)$, to estimate D_R. We find from our simulations that the values of D_R of tracers in this study are not sensitive to the formalism. Figure 8 depicts $U(t)$ (symbols) of icosahedron tracers in Wahnström liquids at different temperatures. Solid lines represent the graph of $\exp(-2D_R t)$ with the value of D_R from the Einstein formalism. Symbols ($U(t)$ for the Debye formalism) and solid lines (obtained from the Einstein formalism) overlap well with each other, indicating that D_R of tracers is not sensitive to the formalism at all temperatures in this study.

We estimate the non-Gaussian parameters ($\alpha_2(t)$) for both the translation and rotation of tracers (Fig. 9). It is interesting that the translational diffusion of tracers follows Gaussian statistics faithfully such that $\alpha_2(t)$ is quite small at all time scales of this study compared to $\alpha_2(t)$ of liquid particles. While $\alpha_2(t)$ of liquid particles reaches up to 1, $\alpha_2(t)$ of the translation of tracer particles are smaller than 0.2. Because the tracer size is comparable to the dynamic domain size of Wahnström and KA liquids, the translational diffusion of tracers is slow and the long time diffusion coefficient may be obtained only after the tracers diffuse through several dynamic domains. The translational diffusion of tracers fails to reflect the heterogeneous dynamics of liquid particles, but instead can be a measure of

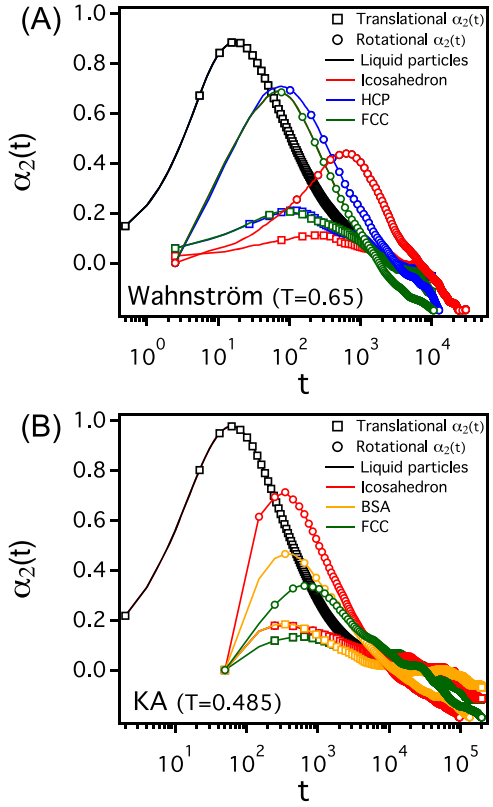

FIG. 9. The non-Gaussian parameters ($\alpha_2(t)$) for the translational diffusion (squares) and the rotational diffusion (circles) of tracers of different structures in (a) Wahnström at $T = 0.65$ and (b) KA liquids at $T = 0.485$. $\alpha_2(t)$ of liquid particles (black squares) is also included.

the overall mobility of the liquids. On the other hand, the rotational diffusion of tracers is quite non-Gaussian with $\alpha_2(t)$ approaching 0.8. This indicates that the rotational diffusion of tracers could reflect the heterogeneous dynamics of liquid particles.

D. Translation-rotation decoupling

The extent of decoupling between the translation and the rotation depends significantly on the shape of tracers. Figure 10(a) depicts the ratio of D_T/D_R normalized by its value at $T = 2$. If both SE and DSE relations were to hold and D_T would couple to D_R, D_T/D_R should stay constant over a range of T. In the case of FCC and HCP tracers in the Wahnström liquid, D_T/D_R stays constant over all temperatures in this study. It is because D_T and D_R of FCC and HCP tracers in the Wahnström liquid follow SE and DSE relations faithfully such that $D_T \sim \tau_T^{-1}$ and $D_R \sim \tau_T^{-1}$ [Fig. 10(b)]. τ_T is the translational relaxation time of tracers obtained from the intermediate scattering function $F(k, t)$ and $F(k, t = \tau_T) = 1/e$, where k denotes the wavevector. $k = 1.85\sigma^{-1}$ and $2.1\sigma^{-1}$ are used for bicapped square antiprism tracers and the other three tracers, respectively. $2\pi/1.85$ and $2\pi/2.1$ correspond to the approximate size of tracers. According to previous studies,[61,62,85–88] τ_T is proportional to η/T, for which τ_T is used to represent η/T in this study. Icosahedron and bicapped square antiprism tracers in the KA liquid also obey SE and DSE relations, for which D_T and D_R couple to each other.

A significant decoupling between D_T and D_R occurs for icosahedron tracers in the Wahnström liquid. Compared to the value of D_T/D_R at $T = 2$, D_T/D_R is increased by a factor of 5 at $T = 0.6$ [Fig. 10(a)]. Such an increase in D_T/D_R at low temperatures suggests two possible scenarios: (1) D_T is enhanced significantly while D_R follows the DSE relation or (2) D_R is suppressed significantly while D_T follows the SE relation. Figure 10(b) depicts D_T and D_R of icosahedron tracers in the Wahnström liquid as a function of τ_T. $D_R \sim \tau_T^{-1.27}$ and $D_T \sim \tau_T^{-1}$, thus implying that the rotational diffusion of icosahedron tracers is significantly hindered in the Wahnström liquid but the translational diffusion follows the SE relation faithfully. The breakdown of the DSE relation for icosahedron tracers leads to the translation-rotation decoupling of icosahedron tracers in the Wahnström liquid.

FCC tracers in the KA liquid also display decoupling between the translation and the rotation, which is not, however, as significant as icosahedron tracers in the Wahnström liquid [Fig. 10(a)]. D_T/D_R at $T = 0.485$ is increased by about a factor of 2 compared to that at $T = 2$. The decoupling occurs for FCC tracers in the KA liquid also because the rotation of FCC tracers is suppressed and $D_R \sim \tau_T^{-1.15}$ while D_T follows the SE relation faithfully [Fig. 10(b)].

E. Local mobility of glass-forming liquids around tracers

Tracers are likely to slow down liquid particles around the tracers, which is expected because tracers may behave as obstacles to the liquid particles. The mobility μ is defined as the average magnitude of displacement of liquid particles during t^*. Here, t^* is the time when the non-Gaussian parameter ($\alpha_2(t)$) of liquid particles becomes maximum and liquid dynamics becomes the most heterogeneous. We estimate the values of μ for all liquid particles ($\mu_{overall}$) in the simulation system and local particles (μ_{local}) around tracers. Local particles are defined as liquid particles that are located within 3σ from the center of mass of tracers. Figure 11 depicts both $\mu_{overall}$ and μ_{local}. The presence of tracers hardly changes $\mu_{overall}$ at all temperatures regardless of the types of tracers. The values of $\mu_{overall}$ are obtained for liquid with and without tracers (of all kinds) and are plotted all together (black symbols) in Figs. 11(a) and 11(b) where different symbols represent different types of tracers in the liquid. The presence of tracers does not change $\mu_{overall}$'s much. Not surprisingly, both $\mu_{overall}$ and μ_{local} decrease upon cooling, and μ_{local} around tracers of any kind is lower than $\mu_{overall}$ (because tracers behave as obstacles to local liquid particles).

In the Wahnström liquid, however, the decrease in μ_{local} around icosahedron tracers is prominent at low temperatures compared to those around other types of tracers. This relates closely to the fact that icosahedron tracers facilitate the formation of icosahedron LFSs around themselves. Because icosahedron LFSs may be stabilized around icosahedron tracers,

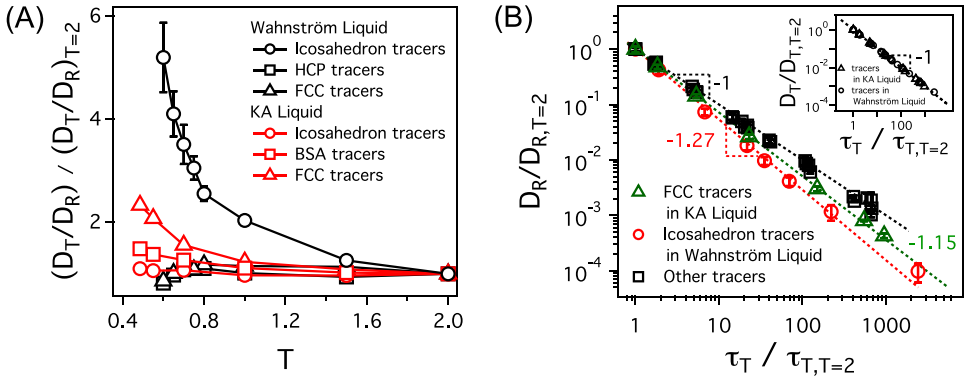

FIG. 10. (a) D_T/D_R normalized by its value at $T = 2$ as a function of T for tracers in Wahnström (black symbols) and KA (red symbols) liquids. (b) D_R normalized by their values at $T = 2$ as a function of τ_T for tracers in Wahnström and KA liquids. Only D_R of icosahedron tracers (red circles) in the Wahnström liquid and FCC tracers (green triangles) in KA liquids are represented with colored symbols. Dotted lines are guides of different exponents. In the inset is D_T normalized by their values at $T = 2$ as a function of τ_T for tracers in Wahnström and KA liquids.

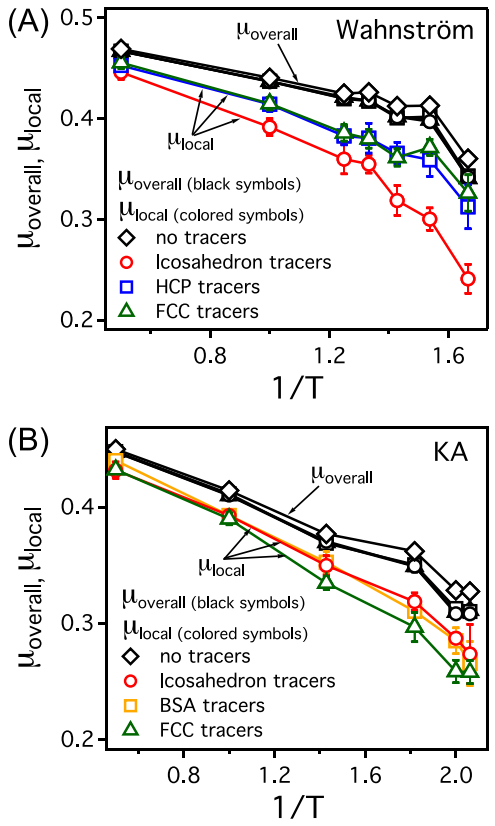

FIG. 11. The overall ($\mu_{overall}$) and local (μ_{local}) mobility of (a) Wahnström particles and (b) KA particles. Black symbols and colored symbols represent $\mu_{overall}$ and μ_{local}, respectively.

any translational motion that may disrupt the icosahedron LFSs would need to overcome a certain free energy barrier. This would slow down the local mobility of liquid particles around icosahedron tracers. The slow-down of local liquid particles around the icosahedron tracers hinders the rotation of the icosahedron tracers, thus breaking down the DSE relation significantly.

Similarly, in the KA liquid, μ_{local} around FCC tracers is suppressed most significantly, which is, however, not as prominent as μ_{local} around icosahedron tracers in the Wahnström liquid. The decrease in μ_{local} around the icosahedron tracers in the Wahnström liquid can be attributed to the facilitation of the icosahedron LFS formation around the icosahedron tracer (as shown in the TCC analysis). However, the FCC tracer in KA liquids does not induce the formation of FCC LFSs (Fig. 5) but still slows down the local mobility of liquid particles around the FCC tracer, thus leading to the breakdown of the DSE relation and the translation-rotation decoupling. It remains unclear how the FCC tracer slows down the local liquid particles and needs to be investigated in a future study.

F. Tracers as stand-ins to interrogate the local mobility around LFSs of glass-forming liquids

Previous simulation studies suggested that icosahedron LFSs in the Wahnström liquid should suppress the mobility of Wahnström particles around icosahedron LFSs, which is consistent with our observation that Wahnström particles are slow around icosahedron tracers.[29,32,48] Hocky *et al.* also performed simulations and reported that the correlation between LFSs and particle mobility was strong in the Wahnström liquid but relatively weak in the KA liquid.[56] This is also in agreement with our results that the translation-rotation decoupling does occur not for bicapped square antiprism tracers in the KA liquid but for icosahedron tracers in the Wahnström liquid. While the translational diffusion of tracers of LFSs obey the SE relation in both Wahnström and KA liquids, their rotational diffusion is dependent on systems: the rotation of icosahedron tracers in the Wahnström liquid is highly suppressed due to the low local mobility, while the rotation of bicapped square antiprism tracers in the KA liquid follows the DSE relation. We also observe in our simulations that μ_{local} around icosahedron tracers in the Wahnström liquid is suppressed significantly, whereas μ_{local} around bicapped square antiprism in the KA liquid is hardly affected, which is also consistent with previous studies.[56] This suggests that the trend of the translation-rotation decoupling of tracers could be associated with the correlation between the LFS domains and the local mobility in glass-forming liquids.

In order to obtain the information on the effect of LFSs, one has to identify LFSs via structural analysis such as TCC and estimate the local mobility using trajectories of particles around the LFSs, which are possible only in molecular simulations. It would be usually infeasible in experiments to identify LFSs and investigate the effect of LFSs on the mobility (and the slow-down of relaxation of glass-forming liquids). Our simulation results suggest that the trend of the translation-rotation decoupling should relate to how the LFS domains and the local mobility would be correlated. Therefore, if one were to measure D_R and D_T and investigate the translation-rotation decoupling of tracers, it could be an indirect approach to investigate the local mobility around LFSs. Because the synthesis of nanoparticles of different structures becomes feasible thanks to advances in nanotechnology, one would be able to observe the translation and rotation of various types of tracers in glass-forming liquids. Even though it would be still challenging to determine LFSs in polymeric and molecular glasses beyond colloidal glasses, the trend of translation-rotation decoupling may still provide information on the heterogeneous dynamics of host liquids.

IV. SUMMARY AND CONCLUSIONS

We perform MD simulations for tracers of different structures in glass-forming liquids to investigate whether the tracers and their translation-rotation decoupling would be used as stand-ins to study the correlation between LFSs and particle mobility. We find from our simulations that the translation-rotation decoupling of tracers depends strongly on the structure of tracers. D_T/D_R of icosahedron tracers in the Wahnström liquid is increased by about a factor of 5 upon cooling, while D_T/D_R of FCC and HCP tracers in the Wahnström liquid stays constant over a whole range of T.

We find from the TCC analysis that icosahedron tracers facilitate the formation of icosahedron LFSs around themselves, which reduces the local mobility around the icosahedron tracers significantly. Such reduced mobility around

icosahedron tracers hinders the rotation of icosahedron tracers, thus resulting in the breakdown of the DSE relation and the fractional viscosity dependence of D_R, i.e., $D_R \sim \tau_T^{-1.27}$. On the other hand, FCC and HCP tracers in the Wahnström liquid do not affect the local structure around those tracers and the decrease in the local mobility is moderate. FCC and HCP tracers, therefore, follow both SE and DSE relations faithfully such that the translation and the rotation of those tracers stay coupled.

Bicapped square antiprism clusters are long-lived LFSs in the KA liquid. We investigate three types of tracers of bicapped square antiprism, icosahedron, and FCC structures in the KA liquid. We find from our simulations that the bicapped square antiprism tracers (that resemble long-lived LFSs in the KA liquid) do not show decoupling behavior even at low temperatures. This is because tracers in the KA liquid do not influence the formation of LFSs around the tracers significantly and the presence of tracers has only a moderate effect on the local mobility around the tracers. Rather, even though FCC tracers do not induce any structural change around tracers, FCC tracers, which are believed to be short-lived structures in the KA liquid, display a moderate decoupling behavior between the translation and the rotation with slow local mobility around tracers and rotational motion compared to other tracers. Our results are consistent with previous simulation results that the correlation between LFSs and particle mobility was relatively weak in the KA liquid.[56]

It is usually not a trivial task to identify LFSs in a glass-forming liquid and elucidate the effects of LFSs on the particle mobility. On the other hand, it becomes feasible to synthesize and design various tracers of the desired structure and size. Therefore, one may investigate the translation-rotation decoupling of various types of tracers in glass-forming liquids not only in simulations but also in experiments. Even though investigating the translation-rotation decoupling would be an indirect route to studying the effects of LFSs on particle mobility, we believe that studying the translation-rotation decoupling of tracers in various glass-forming liquids would shed light on how structural motifs in glass-forming liquids may relate to the particle mobility and slow relaxation of glass-forming liquids.

ACKNOWLEDGMENTS

This work was supported by Samsung Science and Technology Foundation under Project No. SSTF-BA1502-07.

[1] M. D. Ediger, Annu. Rev. Phys. Chem. **51**, 99 (2000).
[2] S. A. Kivelson and G. Tarjus, Nat. Mater. **7**, 831 (2008).
[3] L. Berthier and G. Biroli, Rev. Mod. Phys. **83**, 587 (2011).
[4] M. D. Ediger and P. Harrowell, J. Chem. Phys. **137**, 080901 (2012).
[5] K. Paeng, H. Park, D. T. Hoang, and L. J. Kaufman, Proc. Natl. Acad. Sci. U. S. A. **112**, 4952 (2015).
[6] J. P. Garrahan, Proc. Natl. Acad. Sci. U. S. A. **108**, 4701 (2011).
[7] W. C. K. Poon, MRS Bull. **29**, 96 (2004).
[8] L. Berthier, Physics **4**, 42 (2011).
[9] F. H. Stillinger and P. G. Debenedetti, Annu. Rev. Condens. Matter Phys. **4**, 263 (2013).
[10] K. Kim and S. Saito, J. Chem. Phys. **138**, 12A506 (2013).
[11] N. Lacevic, F. W. Starr, T. B. Schrøder, and S. C. Glotzer, J. Chem. Phys. **119**, 7372 (2003).
[12] P. G. Debenedetti and F. H. Stillinger, Nature **410**, 259 (2001).
[13] G. L. Hunter and E. R. Weeks, Rep. Prog. Phys. **75**, 066501 (2012).
[14] L. Berthier, Phys. Rev. E **69**, 020201 (2004).
[15] E. Flenner, H. Staley, and G. Szamel, Phys. Rev. Lett. **112**, 097801 (2014).
[16] K. Kim, K. Miyazaki, and S. Saito, J. Phys.: Condens. Matter **23**, 234123 (2011).
[17] S. Karmakar, C. Dasgupta, and S. Sastry, Annu. Rev. Condens. Matter Phys. **5**, 255 (2014).
[18] B. R. Parry, I. V. Surovtsev, M. T. Cabeen, C. S. O'Hern, E. R. Dufresne, and C. Jacobs-Wagner, Cell **156**, 183 (2014).
[19] A.-S. Coquel, J.-P. Jacob, M. Primet, A. Demarez, M. Dimiccoli, T. Julou, L. Moisan, A. B. Lindner, and H. Berry, PLoS Comput. Biol. **9**, e1003038 (2013).
[20] S. Bakshi, B. P. Bratton, and J. C. Weisshaar, Biophys. J. **101**, 2535 (2011).
[21] B. P. English, V. Hauryliuk, A. Sanamrad, S. Tankov, N. H. Dekker, and J. Elf, Proc. Natl. Acad. Sci. U. S. A. **108**, E365 (2011).
[22] D. Bi, J. H. Lopez, J. M. Schwarz, and M. L. Manning, Soft Matter **10**, 1885 (2014).
[23] M. Sadati, A. Nourhani, J. J. Fredberg, and N. T. Qazvini, Wiley Interdiscip. Rev.: Syst. Biol. Med. **6**, 137 (2014).
[24] T. E. Angelini, E. Hannezo, X. Trepat, M. Marquez, J. J. Fredberg, and D. A. Weitz, Proc. Natl. Acad. Sci. U. S. A. **108**, 4714 (2011).
[25] Y. Oh, J. Kim, A. Yethiraj, and B. J. Sung, Phys. Rev. E **93**, 012409 (2016).
[26] W. He, H. Song, Y. Su, L. Geng, B. J. Ackerson, H. B. Peng, and P. Tong, Nat. Commun. **7**, 11701 (2016).
[27] F. W. Starr, B. Hartmann, and J. F. Douglas, Soft Matter **10**, 3036 (2014).
[28] E.-M. Schötz, M. Lanio, J. A. Talbot, and M. L. Manning, J. R. Soc. Interface **10**, 20130726 (2013).
[29] A. Malins, J. Eggers, C. P. Royall, S. R. Williams, and H. Tanaka, J. Chem. Phys. **138**, 12A535 (2013).
[30] T. Kawasaki, T. Araki, and H. Tanaka, Phys. Rev. Lett. **99**, 215701 (2007).
[31] A. J. Dunleavy, K. Wiesner, R. Yamamoto, and C. P. Royall, Nat. Commun. **6**, 6089 (2015).
[32] C. P. Royall, S. R. Williams, T. Ohtsuka, and H. Tanaka, Nat. Mater. **7**, 556 (2008).
[33] M. Leocmach and H. Tanaka, Nat. Commun. **3**, 974 (2012).
[34] X. Yang, R. Liu, M. Yang, W.-H. Wang, and K. Chen, Phys. Rev. Lett. **116**, 238003 (2016).
[35] M. Dzugutov, S. I. Simdyankin, and F. H. M. Zetterling, Phys. Rev. Lett. **89**, 195701 (2002).
[36] A. Widmer-Cooper, P. Harrowell, and H. Fynewever, Phys. Rev. Lett. **93**, 135701 (2004).
[37] T. Speck, A. Malins, and C. P. Royall, Phys. Rev. Lett. **109**, 195703 (2012).
[38] P. Chaudhuri, S. Karmakar, and C. Dasgupta, Phys. Rev. Lett. **100**, 125701 (2008).
[39] R. L. Jack, A. J. Dunleavy, and C. P. Royall, Phys. Rev. Lett. **113**, 095703 (2014).
[40] H. Tanaka, T. Kawasaki, H. Shintani, and K. Watanabe, Nat. Mater. **9**, 324 (2010).
[41] T. S. Jain and J. J. de Pablo, J. Chem. Phys. **122**, 174515 (2005).
[42] J. P. Garrahan and D. Chandler, Phys. Rev. Lett. **89**, 035704 (2002).
[43] G. Biroli, Nat. Phys. **3**, 222 (2007).
[44] L. Berthier and J. P. Garrahan, Phys. Rev. E **68**, 041201 (2003).
[45] P. Crowther, F. Turci, and C. P. Royall, J. Chem. Phys. **143**, 044503 (2015).
[46] D. Coslovich, Phys. Rev. E **83**, 051505 (2011).
[47] C. P. Royall, A. Malins, A. J. Dunleavy, and R. Pinney, J. Non-Cryst. Solids **407**, 34 (2015).
[48] A. Malins, J. Eggers, H. Tanaka, and C. P. Royall, Faraday Discuss. **167**, 405 (2013).
[49] H. Shintani and H. Tanaka, Nat. Phys. **2**, 200 (2006).
[50] F. Sausset and G. Tarjus, Phys. Rev. Lett. **104**, 065701 (2010).
[51] C. P. Royall and W. Kob, J. Stat. Mech.: Theory Exp. **2017**, 024001.
[52] C. P. Royall and S. R. Williams, Phys. Rep. **560**, 1 (2015).
[53] D. Coslovich and G. Pastore, J. Chem. Phys. **127**, 124504 (2007).
[54] U. R. Pedersen, T. B. Schrøder, J. C. Dyre, and P. Harrowell, Phys. Rev. Lett. **104**, 105701 (2010).
[55] S. Karmakar, C. Dasgupta, and S. Sastry, Rep. Prog. Phys. **79**, 016601 (2016).
[56] G. M. Hocky, D. Coslovich, A. Ikeda, and D. R. Reichman, Phys. Rev. Lett. **113**, 157801 (2014).
[57] K. V. Edmond, M. T. Elsesser, G. L. Hunter, D. J. Pine, and E. R. Weeks, Proc. Natl. Acad. Sci. U. S. A. **109**, 17891 (2012).
[58] F. H. Stillinger and J. A. Hodgdon, Phys. Rev. E **50**, 2064 (1994).
[59] G. Tarjus and D. Kivelson, J. Chem. Phys. **103**, 3071 (1995).
[60] S.-H. Chong and W. Kob, Phys. Rev. Lett. **102**, 025702 (2009).

[61]T. G. Lombardo, P. G. Debenedetti, and F. H. Stillinger, J. Chem. Phys. **125**, 174507 (2006).
[62]M. G. Mazza, N. Giovambattista, H. E. Stanley, and F. W. Starr, Phys. Rev. E **76**, 031203 (2007).
[63]M. Roos, M. Ott, M. Hofmann, S. Link, E. Rössler, J. Balbach, A. Krushelnitsky, and K. Saalwächter, J. Am. Chem. Soc. **138**, 10365 (2016).
[64]Y. Wang, C. Li, and G. J. Pielak, J. Am. Chem. Soc. **132**, 9392 (2010).
[65]A. Krushelnitsky, Phys. Chem. Chem. Phys. **8**, 2117 (2006).
[66]G. H. Koenderink, H. Zhang, D. G. A. L. Aarts, M. P. Lettinga, A. P. Philipse, and G. Nägele, Faraday Discuss. **123**, 335 (2003).
[67]S. Zorrilla, M. A. Hink, A. J. Visser, and M. P. Lillo, Biophys. Chem. **125**, 298 (2007).
[68]G. Tarjus, S. A. Kivelson, Z. Nussinov, and P. Viot, J. Phys.: Condens. Matter **17**, R1143 (2005).
[69]V. N. Manoharan and D. J. Pine, MRS Bull. **29**, 91 (2004).
[70]J. Kim, C. Kim, and B. J. Sung, Phys. Rev. Lett. **110**, 047801 (2013).
[71]D. A. Stariolo and G. Fabricius, J. Chem. Phys. **125**, 064505 (2006).
[72]M. Saadatfar and M. Sahimi, Phys. Rev. E **65**, 036116 (2002).
[73]G. Kwon, B. J. Sung, and A. Yethiraj, J. Phys. Chem. B **118**, 8128 (2014).
[74]J. Guan, B. Wang, and S. Granick, ACS Nano **8**, 3331 (2014).
[75]G. Szamel and E. Flenner, Phys. Rev. E **73**, 011504 (2006).
[76]B. Wang, J. Kuo, S. C. Bae, and S. Granick, Nat. Mater. **11**, 481 (2012).
[77]G. Wahnström, Phys. Rev. A **44**, 3752 (1991).
[78]W. Kob, C. Donati, S. J. Plimpton, P. H. Poole, and S. C. Glotzer, Phys. Rev. Lett. **79**, 2827 (1997).
[79]W. Kob and H. C. Andersen, Phys. Rev. E **51**, 4626 (1995).
[80]W. Kob and H. C. Andersen, Phys. Rev. E **52**, 4134 (1995).
[81]H. Arkin and W. Janke, J. Chem. Phys. **138**, 054904 (2013).
[82]See https://lammps.sandia.gov for the information about LAMMPS molecular dynamics simulator.
[83]A. Malins, S. R. Williams, J. Eggers, and C. P. Royall, J. Chem. Phys. **139**, 234506 (2013).
[84]S. Taamalli, H. Belmabrouk, V. V. Hoang, and V. Teboul, Chem. Phys. **490**, 55 (2017).
[85]S. Sengupta, S. Karmakar, C. Dasgupta, and S. Sastry, J. Chem. Phys. **138**, 12A548 (2013).
[86]Y. Jung, J. P. Garrahan, and D. Chandler, Phys. Rev. E **69**, 061205 (2004).
[87]C. D. Michele and D. Leporini, Phys. Rev. E **63**, 036701 (2001).
[88]E. H. Grant, J. Chem. Phys. **26**, 1575 (1957).